THE JOURNAL OF BIOLOGICAL CHEMISTRY VOL. 288, NO. 27, pp. 19401–19413, July 5, 2013
Published in the U.S.A.

Translational Redefinition of UGA Codons Is Regulated by Selenium Availability*[S]

Received for publication, April 26, 2013, and in revised form, May 17, 2013 Published, JBC Papers in Press, May 21, 2013, DOI 10.1074/jbc.M113.481051

Michael T. Howard[‡1], **Bradley A. Carlson**[§], **Christine B. Anderson**[‡], **and Dolph L. Hatfield**[§]

From the [‡]*Department of Human Genetics, University of Utah, Salt Lake City, Utah 84112 and* [§]*Molecular Biology of Selenium Section, Laboratory of Cancer Prevention, Center for Cancer Research, NCI, National Institutes of Health, Bethesda, Maryland 20892*

Background: Selenium is incorporated into selenoproteins as the amino acid, selenocysteine.
Results: Dietary selenium supplementation increases ribosome density downstream of selenocysteine-encoding UGA codons.
Conclusion: Dietary selenium levels differentially regulate selenoprotein expression by controlling the rate-limiting step of selenocysteine incorporation.
Significance: The mechanisms by which dietary selenium can affect the readout of the genetic code and selenoprotein expression have been illuminated.

Incorporation of selenium into ~25 mammalian selenoproteins occurs by translational recoding whereby in-frame UGA codons are redefined to encode the selenium containing amino acid, selenocysteine (Sec). Here we applied ribosome profiling to examine the effect of dietary selenium levels on the translational mechanisms controlling selenoprotein synthesis in mouse liver. Dietary selenium levels were shown to control gene-specific selenoprotein expression primarily at the translation level by differential regulation of UGA redefinition and Sec incorporation efficiency, although effects on translation initiation and mRNA abundance were also observed. Direct evidence is presented that increasing dietary selenium causes a vast increase in ribosome density downstream of UGA-Sec codons for a subset of selenoprotein mRNAs and that the selenium-dependent effects on Sec incorporation efficiency are mediated in part by the degree of Sec-tRNA$^{[Ser]Sec}$ Um34 methylation. Furthermore, we find evidence for translation in the 5′-UTRs for a subset of selenoproteins and for ribosome pausing near the UGA-Sec codon in those mRNAs encoding the selenoproteins most affected by selenium availability. These data illustrate how dietary levels of the trace element selenium can alter the readout of the genetic code to affect the expression of an entire class of proteins.

Selenium is a naturally occurring trace element that is essential for human health in small amounts but toxic at high levels. Human diseases associated with extreme selenium deficiency have been identified in geographic regions that are very low in selenium soil content, *e.g.* Keshan disease, a regional cardiomyopathy, which is endemic in regions of China (1). In regions of high selenium soil content, selenium toxicity can manifest as a condition called selenosis that is characterized by gastrointestinal upset, hair loss, fatigue, mood changes, and nerve damage (2, 3). Although disease symptoms resulting from severe selenium deficiency or intoxication are rare, there is strong evidence that less-overt variations in selenium status have multifaceted health effects including the risk of cancer, diabetes, skeletal muscle, and cardiac disease as well as maintenance of proper immune function (4).

One well established role of selenium is its incorporation into ~25 mammalian selenoproteins as the amino acid, selenocysteine (Sec)[2] (5, 6). This is accomplished by an expansion of the normal rules of decoding to allow UGA codons to encode Sec in addition to its normal role in terminating translation. Ribosome reprogramming and the process of UGA-Sec codon redefinition is orchestrated by cis-acting Sec insertion sequence (SECIS) elements that reside in the 3′-UTR of selenoprotein mRNAs (7–10), as well as trans-acting factors including the SECIS-binding protein, SBP2 (11), and the Sec-specific elongation factor, eEFSec (12, 13), which ultimately delivers Sec-tRNA$^{[Ser]Sec}$ to the ribosome (4).

In the context of selenoproteins, Sec mediates reductive/oxidation reactions on a number of substrates important for cellular redox homeostasis, thyroid hormone metabolism, protein folding, and disulfide formation or isomerization (4). It is also known that selenium availability can have a profound effect on selenoprotein levels with synthesis of certain essential housekeeping selenoproteins, thioredoxin reductase 1 (Txnrd1) and glutathione peroxidase 4 (Gpx4), for example, being more resistant to selenium limitation than stress-related selenoproteins, such as glutathione peroxidase 1 (Gpx1) (14–16). The "hierarchy" of differential selenoprotein expression in response to selenium availability and the specific substrates

* This work was supported, in whole or in part, by the National Institutes of Health (NIH Grant R21ES022716; to M. T. H.) and the Intramural Research Program of the NIH, NCI, Center for Cancer Research (to D. L. H.). This work was also supported by a University of Utah Seed grant (to M. T. H.).
[S] This article contains supplemental Figs. S1–S3.
[1] To whom correspondence should be addressed. Tel.: 801-585-1927; E-mail: mhoward@genetics.utah.edu.

[2] The abbreviations used are: Sec, selenocysteine; RPF, ribosome-protected fragment; UGA-Sec, UGA selenocysteine codon; SECIS, Sec insertion sequence element; NMD, nonsense-mediated decay; mcm^{5}U, 5-methoxycarbonylmethyluridine; mcm^{5}Um, 5-methoxycarbonylmethyl-2′-*O*-methyluridine; RPFKM, reads per kilobase per million mapped reads for ribosome footprints; RPKM, reads per kilobase per million mapped reads for total RNA; CDS, coding sequence; Txnrd1, thioredoxin reductase 1; Gpx4, glutathione peroxidase 4; TE, translational efficiency; nt, nucleotides.

and biochemical pathways affected likely account for the diversity of health effects associated with dietary selenium intake.

Despite the identification of key components of selenocysteine synthesis and incorporation, the mechanism by which dietary selenium affects selenoprotein synthesis remains controversial. One commonly invoked mechanism involves the nonsense-mediated decay (NMD) pathway in which, under selenium limiting conditions, the UGA-Sec codon in nonessential selenoprotein messages is recognized as a premature termination codon causing RNA degradation. For example, the reduction of *Gpx1* mRNA levels under selenium deficiency has been shown to be due to post-transcriptional mRNA turnover rather than reduced transcription (17) by induction of the NMD pathway (18, 19), whereas *Gpx4* mRNA levels are unaffected and resistant to NMD. Other explanations implicate changes in Sec insertion efficiency during translation due to differences in SECIS elements and their ability to recruit the Sec incorporation machinery (20–22). Also, it is known that selenium levels directly correlate with the degree of Um34 methylation of Sec-tRNA$^{[Ser]Sec}$ wherein the Sec-tRNA$^{[Ser]Sec}$ population consists of two isoforms, the non-Um34-containing isoform, 5-methoxycarbonylmethyluridine (mcm^{5}U), and the Um34-containing isoform, 5-methoxycarbonylmethyl-2′-*O*-methyluridine (mcm^{5}Um) (23). Based on the observation that the mcm^{5}Um isoform is required for efficient expression of the stress-related selenoproteins but not for the housekeeping selenoproteins, it has been proposed that differential utilization of the two Sec-tRNA$^{[Ser]Sec}$ isoforms during translation of selenoprotein mRNAs could account for selenium regulation of selenoprotein synthesis (24–26). Together these studies suggest that biosynthesis of selenoproteins is a complex process that may involve multiple levels of control; however, the degree of which each process may contribute to selenium-dependent regulation is unknown.

To directly examine the mechanisms of selenium-dependent regulation of selenoprotein expression *in vivo*, we have applied ribosome profiling, RNA-Seq, and traditional biochemical approaches to examine selenoprotein synthesis in liver. Using these approaches, we have defined the changes in mRNA abundance and translational activity that occur in response to altered dietary selenium intake and expression of a mutant Sec-tRNA$^{[Ser]Sec}$ that prevents Um34 synthesis. Quantitative mapping of ribosome distribution at nucleotide resolution on selenoprotein mRNAs revealed that translational control of selenoprotein synthesis occurred primarily due to changes in Sec incorporation efficiency. Furthermore, translation of *Gpx1*, *Sepx1*, *Sepw1*, and *Selh* mRNAs requires the Sec-tRNA$^{[Ser]Sec}$ mcm^{5}Um isoform for efficient UGA-Sec decoding and involves an excess of ribosome protection upstream or at the UGA-Sec codon. Finally, we find an excess of ribosome-protected fragments upstream of the initiation codons for *Selh*, *Sephs2*, *Txnrd1*, and *Selt*. These studies provide a unique view of selenoprotein translational control and UGA redefinition efficiency in mammalian tissue and its regulation by dietary selenium intake.

EXPERIMENTAL PROCEDURES

Lysate Preparation—Three-week-old male WT and *Trsp*^{A37G} mice in a FVB/N background were fed diets supplemented with 0, 0.1, and 2.0 ppm selenium diets for 6 weeks before euthanasia. All animal work was approved under National Institutes of Health Institutional Animal Care and Use Committees protocol BRL-002. Livers were rapidly excised, cut into four equal parts, and immediately frozen in liquid nitrogen. For each experiment, 100 mg of frozen tissue was placed in a 2-ml tube containing a ¼-inch-diameter stainless steel ball with 1.5 ml of pre-chilled lysis buffer (10 mM Tris-Cl (pH 7.5), 300 mM KCl, 10 mM $MgCl_2$, 200 μg/ml cycloheximide (Sigma), 1 mM DTT, and 1% Triton X-100). Samples were homogenized by agitation at full speed for 45 s in the Mini-Beadbeater-8 (Biospec Products, Inc.).

Ribonuclease Digestion and Total RNA Preparation—To minimize biological variation, total RNA for RNA-Seq analysis and ribosome-protected fragments were prepared from the same lysate. 300 μl of crude lysate were immediately transferred to 2 ml of TRIzol reagent (Invitrogen), and total RNA was extracted according to the manufacturer's specification. The remaining lysate was incubated with 500 units of RNase I (Invitrogen) for 30 min at 25 °C. Monosomes were isolated by centrifugation at 48,000 rpm for 2 h in a TL100 ultracentrifugation (Beckman Coulter). Ribonuclease-resistant RNA fragments were isolated from the pellet by TRIzol extraction and electrophoresed on a 15% polyacrylamide, 8 M urea gel. The region of the gel containing 26–36-nucleotide-size RNA fragments was excised, and RNA was isolated by passive elution before library construction.

Ribosome Profiling and Library Construction—Gel-purified ribosome footprints and hydrolyzed total RNA fragments were treated with 5 units of Antarctic phosphatase (New England Biolabs) in the presence of 40 units of RNase inhibitor (Ambion) for 30 min at 37 °C followed by 5 min at 65 °C to deactivate the enzyme. Fragments were then treated with 20 units of polynucleotide kinase (New England Biolabs) for 60 min at 37 °C and purified using RNeasy MinElute columns (Qiagen) according to the manufacturer's recommendations for small RNA. RPF and total RNA libraries were built using the TruSeq Small RNA Sample preparation kit (Illumina) according to the manufacturer's specifications with rRNA subtraction using Ribo-Zero (Epicenter). Limited PCR was used to enrich for ligated fragments.

Illumina Sequencing and Processing of Reads—Library aliquots were run on an Agilent 2100 DNA high sensitivity bioanalyzer chip to validate the library size range. RPF and total RNA libraries were subjected to 50 cycles of single-end sequencing on an Illumina HiSeq 2000 instrument. Adapter sequences were removed using the Hannon laboratory FastX toolkit. rRNA sequences were removed using bowtie (27) alignment against mouse rRNA sequences, and all unaligned sequences were retained for further processing.

Alignment to RefSeq mRNA Sequences—RefSeq fasta sequences were obtained from the UCSC genome browser (mm9 assembly, RefSeq Genes were downloaded in November of 2012). These fasta files were reduced to a single entry for each

mRNA corresponding to the longest transcript isoform. For CDS alignments, the first 15 and last 3 codons were excluded to avoid bias caused by altered footprint density at the initiation and termination codons. Sequences that aligned to only a single site within the database, allowing for two mismatches, were identified using the bowtie short sequence aligner (27). Technical variability was addressed by linear regression analysis of all RefSeq mRNAs with greater than 0.01 RPFKM or RPKM values (11,918 mRNAs) for WT samples obtained from mice fed diets supplemented with 0.1 or 2.0 ppm selenium. In each comparison R^2 values were >0.98, and >92% of mRNAs revealed less than a 2-fold difference in RPFKM or RPKM values (data not shown).

Ribosome profiling and total RNA sequences were aligned separately to selenoprotein and *Gapdh* mRNAs and were determined using the bowtie alignment parameters described above against the following RefSeq entries: NM_027652.2 *Seli*, NM_027905 *Selo*, NM_007860.3 *Dio1*, NM_013759.2 *Sepx1*, NM_024439.3 *Sels*, NM_015762.2 *Txnrd1*, NM_008160.6 *Gpx1*, NM_008162.2 *Gpx4*, NM_009155.3 *Sepp1*, NM_053102.2 *Sep15*, NM_013711.3 *Txnrd2*, NM_019979.2 *Selk*, NM_001040396.2 *Selt*, NM_009156.2 *Sepw1*, NM_009266.3 *Sephs2*, NM_030677.2 *Gpx2*, NM_001178058.1 *Txnrd3*, NM_029100.2 *Sepn1*, NM_053267.2 *Selm*, NM_008161.3 *Gpx3*, NM_001033166.2 *Selh*, NM_172119.2 *Dio3*, NM_010050.2 *Dio2*, NM_175033.3 *Selv*, NM_008084.2 *Gapdh*.

Quantitative Analysis and A-site Assignment—The 5′ end of ribosome profiling and RNA reads were offset to the predicted first nucleotide of the A-site using the following rule: for sequence lengths ≤34 nt (+17 nt from the 5′ end of the sequence) and for sequence lengths ≥35 nt (+18 nt from the 5′ end of the sequence). These values were determined as the optimum to position initiating ribosome P-sites at the AUG codon for all RefSeq mRNAs (see supplemental Figs. S1 and S3). Total mapped reads used to derive RPKM calculation were determined by aligning sequences to the CDSs of the RefSeq database described above. Total number of aligned reads were: WT 0 ppm selenium 23,945,053 (ribosome profiling) and 16,709,701 (RNA); WT 0.1 ppm selenium 30,296,837 (ribosome profiling) and 14,220,047 (RNA); WT 2.0 ppm selenium 17,763,406 (ribosome profiling) and 12,399,318 (RNA); *Trsp*^{A37G} 0 ppm selenium 28,864,210 (ribosome profiling) and 12,403,067 (RNA); *Trsp*^{A37G} 0.1 ppm selenium 29,816,461 (ribosome profiling) and 10,669,213 (RNA); *Trsp*^{A37G} 2.0 ppm 22,139,115 (ribosome profiling) and 13,073,779 (RNA). Analysis of ribosome footprinting upstream of the UGA-Sec codon excluded the first 15 codons after the initiation codon and the 5 codons preceding the UGA-Sec codon. Ribosome footprinting RPKMs downstream of the UGA-Sec were calculated from the second codon after UGA-Sec to the third codon preceding the stop codon. For reads assigned to A-site codons (Fig. 6 and supplemental Fig. S3), only ribosome footprints of 32 to 36 nt were utilized. The reads that mapped to the first nucleotide of a codon were then summed with those mapping to the adjacent −1 and +1 nucleotide positions to determine the number of footprints with A-sites assigned to each codon.

Western Blot Analysis—Protein extracts were prepared from WT and *Trsp*^{A37G} mouse liver (n = 2) by homogenizing the liver in ice-cold lysis buffer (50 mM Tris (pH 7.5), 150 mM NaCl, 1 mM EDTA, 0.1% Igepal, and Complete Mini Protease Inhibitor (Roche Applied Science)). Total protein was electrophoresed on 4–12% NuPage polyacrylamide gels (Invitrogen), transferred onto PVDF membranes (Bio-Rad), and blotted with antibodies against Txnrd1, Gpx4, Sep15 (Epitomics), Gpx1 (Abcam), Sepw1 (Rockland), Sepx1 or Selt (26). After incubation of the primary antibody, membranes were washed with TBS-T (Tris-buffered saline; 20 mM Tris/HCl (pH 7.5), 150 mM NaCl containing 0.1% Tween 20) and incubated in anti-rabbit HRP-conjugated secondary antibody (Thermo Scientific). Membranes were washed with TBS-T, incubated in Supersignal West Dura Extended Duration Substrate (Thermo Scientific), and exposed to x-ray film.

Quantitative PCR—Total RNA was isolated from WT and *Trsp*^{A37G} mouse liver (n = 3) using TRIzol (Invitrogen), and two-step quantitative real-time-PCR was performed to determine the relative expression of genes using the primer sequences as given (28). For each sample, total RNA (1 μg) was reverse-transcribed using an iScript cDNA Synthesis kit (Bio-Rad) according to the vendor's instructions and used for quantitative real-time-PCR using DyNAmo SYBR Green (Thermo Scientific). Reactions were carried out in triplicate, and RNA levels were normalized to *Gapdh*.

RESULTS

Selenium-deficient Availability and Sec-tRNA$^{[Ser]Sec}$ *Um34 Modification Affect Global Translation of the Selenoproteome*—Ribosome profiling involves the isolation and deep sequencing of ribosome-protected fragments (ribosome footprints or RPFs) after digestion of unprotected mRNA with RNase1 (29–31). Ribosome density and position on thousands of mRNAs can be determined by quantification and localization of ribosome footprints. An alternative method involving sucrose gradient fractionation of intact polysomes and microarray hybridization to determine mRNA position in the gradient was developed previously and applied to estimate overall ribosome density on mRNAs (32, 33). However, we selected ribosome profiling for analyzing selenoprotein expression due to its ability to measure both mRNA ribosome density and ribosome position at codon resolution. As previous *in vitro* studies have shown that UGA redefinition to encode Sec is in competition with termination (34, 35), we postulated that the ability to quantify ribosomes located 5′ and 3′ of UGA-Sec codons would provide a means of estimating changes in Sec incorporation efficiency and a more accurate method for measuring changes in full-length selenoprotein synthesis. Herein, we have applied this technique to examine the effects of altered dietary selenium levels and Sec-tRNA$^{[Ser]Sec}$ modification status on synthesis of the liver selenoproteome as outlined in Fig. 1*A*.

Um34 synthesis is the last step in maturation of tRNA$^{[Ser]Sec}$ and is dependent on an intact tertiary structure (36), prior synthesis of all base modifications, including isopentenyladenosine at position 37 (24, 26), and aminoacylation of the tRNA (37). When mammalian cells or tissues are selenium-deficient, the mcm^{5}U isoform is enriched relative to the mcm^{5}Um isoform, whereas the opposite is true under selenium sufficiency (Fig. 1*B*). A37G prevents Um34 synthesis (24, 26). The *Trsp*^{A37G}

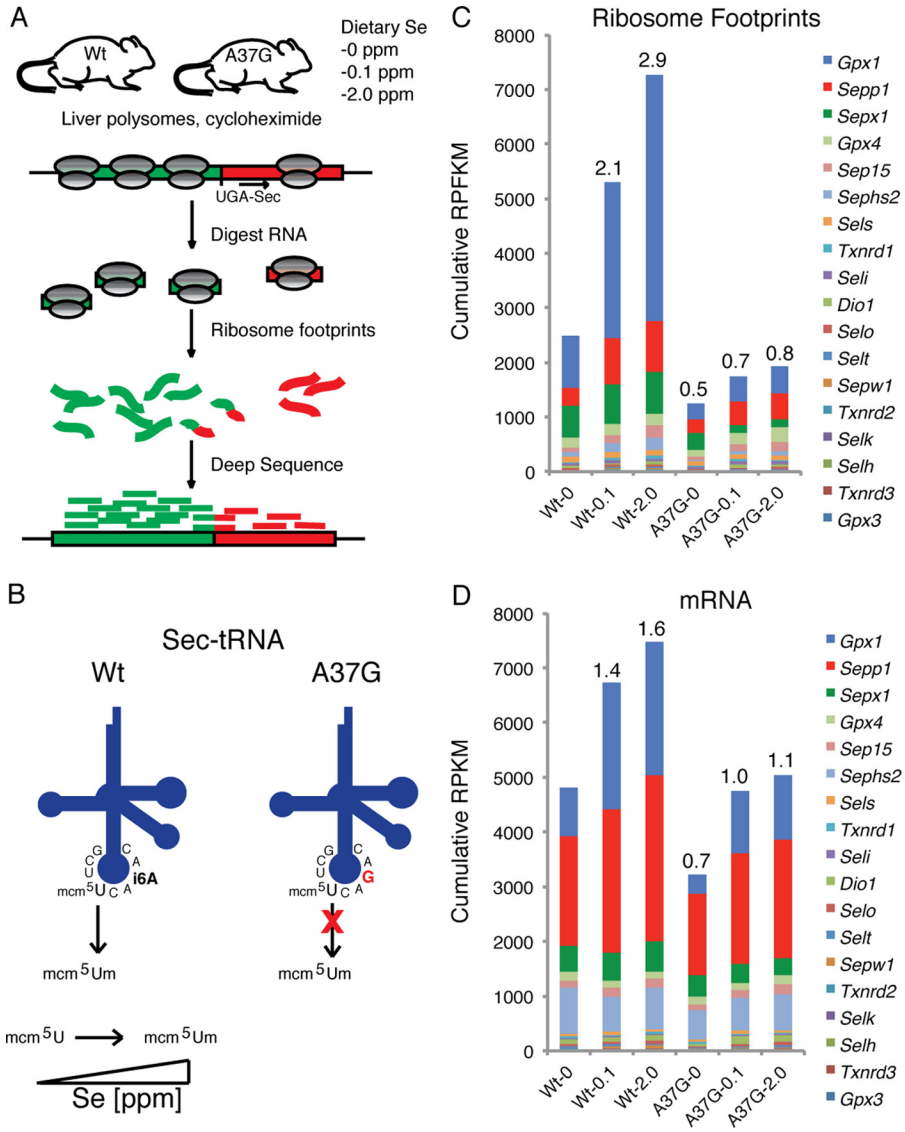

FIGURE 1. **Overview of experimental design and changes in global selenoproteome synthesis as a function of dietary selenium and Um34 methylation of Sec-tRNA$^{[Ser]Sec}$.** *A*, livers were harvested from WT mice and *Trsp*^{A37G} transgenic mice (A37G) fed diets supplemented with 0, 0.1, or 2.0 ppm selenium. Liver tissue was subjected to ribosome profiling, deep sequencing, and alignment to selenoprotein mRNAs. *B*, a schematic shows WT tRNA$^{[Ser]Sec}$ and A37G tRNA$^{[Ser]Sec}$ in a cloverleaf model with the base sequence in the anticodon loop and locations of mcm^{5}U, mcm^{5}Um, isopentenyladenosine, and A37G indicated. Increasing dietary selenium levels enhance Um34 synthesis, whereas the A37G change prevents Um34 synthesis. *C*, shown is the cumulative fraction of ribosome footprints (RPFKM, ribosome footprint/kilobase/million mapped reads) mapping to each selenoprotein mRNA coding sequence. *D*, shown is the cumulative fraction of RNA sequence reads (RPKM, RNA reads/kilobase/million mapped reads) mapping to each selenoprotein mRNA. The fold change relative to WT mice fed selenium-deficient diets is shown *above each column* in *C* and *D*.

transgenic mouse, which encodes 20 copies of the A37G transgene generates a Sec-tRNA$^{[Ser]Sec}$ population consisting of a much higher proportion of mutant than wild type tRNA$^{[Ser]Sec}$ (24).

We fed WT and *Trsp*^{A37G} mice defined diets supplemented with 0, 0.1, or 2.0 ppm selenium. Livers were harvested, and ribosome profiling experiments were performed as described under "Experimental Procedures." Undigested total RNA was processed for RNA-Seq in parallel to estimate changes in mRNA abundance. Ribosome-protected fragments and total RNA fragments were aligned to an mRNA database derived from RefSeq. Analysis of tissue-derived ribosome footprint mRNA alignments to all CDSs longer than 1000 nt (supplemental Fig. S1*A*) revealed, as expected, that ribosome footprints were highly enriched in CDSs relative to the UTRs, and strong triplet phasing was observed corresponding to the step size of the ribosome. Importantly, no global bias was observed in the average ribosome protection toward the 3′ end of CDSs, indicating ribosomes were rapidly captured during tissue lysis. As has been previously reported (29, 31), a number of RPFs mapped to 5′-UTRs, likely reflecting ribosome occupancy of upstream open reading frames, and there was an elevation in RPFs found near the initiation codon. Thus, we show here that ribosome profiling in intact mammalian tissue captures the expected features of actively translating ribosomes.

The effects of altered dietary selenium and Sec-tRNA$^{[Ser]Sec}$ modification on translation and mRNA abundance of the selenoproteome were examined by aligning ribosome footprint or total RNA sequence reads to the mRNA reference sequences for all 24 selenoproteins in mice. Ribosome density and mRNA

abundance were assessed by counting the number of reads mapping to each mRNA corrected for the mRNA length and normalized to the total mapped reads for each sample (reads per kilobase per million mapped reads: RPFKM for ribosome footprints and RPKM for total RNA fragments) (38). The global effect of dietary selenium levels on ribosome activity and mRNA abundance across the selenoproteome is shown as the cumulative ribosome footprint RPFKM (Fig. 1*C*) and mRNA RPKM (Fig. 1*D*) for all selenoproteins with greater than 25 mapped ribosome-protected fragments or mRNA sequences in the sample derived from WT mice fed diets supplemented with 0.1 ppm selenium. The addition of 0.1 or 2.0 ppm selenium to the diets of WT mice increased global selenoprotein translation and mRNA abundance compared with the levels seen in mice fed selenium-deficient diets. Selenoprotein translational activity, mRNA abundance, and magnitude of response to increased dietary selenium were reduced in $Trsp^{A37G}$ mice. Although both mRNA abundance and translational activity of the selenoproteome were affected, the greatest changes in response to increased dietary selenium levels in WT mice (~2–3×) was observed for ribosome footprint RPFKMs, demonstrating that translational control plays a central role in the selenium-dependent regulation of the liver selenoproteome.

Selenium Availability and A37G Sec-tRNA$^{[Ser]Sec}$ Have Gene-specific Effects on Selenoprotein mRNA Abundance and Ribosome Density—We applied RNA-Seq to quantify selenoprotein mRNA abundance as a function of dietary selenium and Um34 methylation. The RNA RPKM measurements were first validated by comparison to quantitative real-time PCR (see supplemental Fig. S2). RPKM and quantitative real-time PCR measurements for the selenoprotein mRNAs in each sample were highly correlated ($r > 0.95$). Selenoprotein mRNA levels (Fig. 2*A*) span nearly 3 orders of magnitude with selenoprotein P *(Sepp1)*, *Gpx1*, selenophosphate synthetase 2 *(Sephs2)*, and *Sepx1* being highly abundant in mouse liver. In WT mice, *Gpx1*, *Sepw1*, and selenoprotein H (*Selh*) mRNA levels were most sensitive to dietary selenium availability with the addition of 0.1 or 2.0 ppm selenium to diets, resulting in a >2-fold increase in mRNA abundance (Fig. 2*C* and supplemental Fig. S2). In selenium-deficient $Trsp^{A37G}$ mice, the abundance of these three mRNAs was reduced relative to that seen in selenium-deficient WT mice, and RNA levels were restored to varying degrees by the addition of selenium to the diet. Deiodinase 1 (*Dio1*) showed a marked decrease in mRNA abundance in selenium-deficient $Trsp^{A37G}$ mice that was increased by ~5-fold in the $Trsp^{A37G}$ mutants fed selenium- supplemented diets. An effect of this magnitude on *Dio1* mRNA was not observed in samples from WT mice.

Next we examined translational activity on selenoprotein mRNAs. As Sec incorporation efficiency is not 100%, we surmised that ribosome density downstream of the UGA-Sec codon would provide the most accurate measure of translational activity leading to the production of full-length protein. CDS RPFKM measurements downstream of the UGA-Sec codon are shown in Fig. 2*B* and supplemental Fig. S2. For some selenoprotein mRNAs, the UGA-Sec codon is near the 3′ end of the CDS (selenoprotein S (*Sels*), selenoprotein O (*Selo*), *Txnrd1*, *Txnrd2*, *Txnrd3*, and selenoprotein K (*Selk*)). In these cases, ribosome footprint RPFKMs were calculated for the entire CDS and, consequently, may not reflect the production of functional full-length Sec-containing protein due to the fraction of ribosomes that may terminate at the UGA-Sec codon. For all selenoproteins with non-C-terminal UGA-Sec codons with the exception of *Seli* (discussed below) and *Gpx3*, there was an increase in RPFKMs downstream of the UGA-Sec codon in WT mice that ranged from ~2 to nearly 30-fold in mice fed selenium supplemented diets relative to those on selenium-deficient diets (Fig. 2*D*). The largest increases were seen for *Gpx1* (13× and 16×), *Sepx1* (6× and 8×), *Sepw1* (7× and 11×), and *Selh* (21× and 27×). Similarly, selenium addition to the diets of $Trsp^{A37G}$ mice resulted in an increase in 3′ ribosome footprint RPFKMs, although in many cases to a lesser extent than seen in WT mice. Notably, there was a substantial reduction in the total RPFKMs in $Trsp^{A37G}$ mice fed selenium-supplemented diets relative to their WT counterparts for *Gpx1*, *Sepx1*, *Sepw1*, *Selh* (and to a lesser extent for *Sepp1*, *Sephs2*, *Selenoprotein T* (*Selt*), and *Gpx3*), suggesting that Um34 methylation was required to varying degrees for efficient synthesis of these selenoproteins. In contrast, 3′ RPFKMs in $Trsp^{A37G}$ mice were restored to WT levels by selenium supplementation for *Gpx4*, *Sep15*, and *Dio1.*

The relative selenium-dependent change in abundance of the three proteins in which 3′ RPFKMs were significantly reduced in the $Trsp^{A37G}$ mutant (Gpx1, Sepw1, Sepx1) and four where RPFKMs were unaffected or affected to a lesser degree (Gpx4, Sep15, Selt, Txnrd1) was determined by Western blot analysis (Fig. 3). Comparisons to the changes in RPFKMs confirmed qualitatively similar results supporting the validity of utilizing ribosome profiling to approximate changes in selenoprotein levels.

Sec Incorporation Efficiency Accounts for the Selenium-dependent Translational Control of Selenoprotein Synthesis—Ribosome footprint RPFKMs reflect the number of ribosomes actively synthesizing protein for each mRNA, whereas translational efficiency (TE) (the amount of ribosome footprints normalized to mRNA abundance, RPFKM/RPKM) provides a means of estimating translational regulation. In Fig. 4*A*, the TE across the CDS is shown for abundant selenoproteins in liver. A broad range of TEs is observed with *Seli*, *Sels*, and *Txnrd2*, examples of selenoprotein mRNAs with apparent high translational efficiency (see below), whereas *Sepp1*, *Sephs2*, and *Sepw1* mRNAs are mRNAs that appear to have low translational efficiency. Assuming that the average translation elongation rate preceding and following the UGA-Sec codon is constant, CDS TE is primarily determined by both the efficiency of translation initiation and the efficiency of Sec insertion. As Sec incorporation efficiency is not 100% and it is conceivable that slow decoding of the UGA-Sec codon could slow the elongation rates of upstream ribosomes, the overall CDS TE may be strongly influenced by both the efficiency of Sec incorporation and the position of the UGA-Sec codon within the CDS (Fig. 4*B*), thus making interpretation of whole CDS RPFKM values challenging. To circumvent these limitations, we determined the TE for regions upstream (5′ TE) and downstream (3′ TE) of the UGA-Sec codon, independently. However, for some selenoproteins it was not possible to obtain TE measurements either because the UGA-Sec codon was too near the 5′ or 3′ ends or the interro-

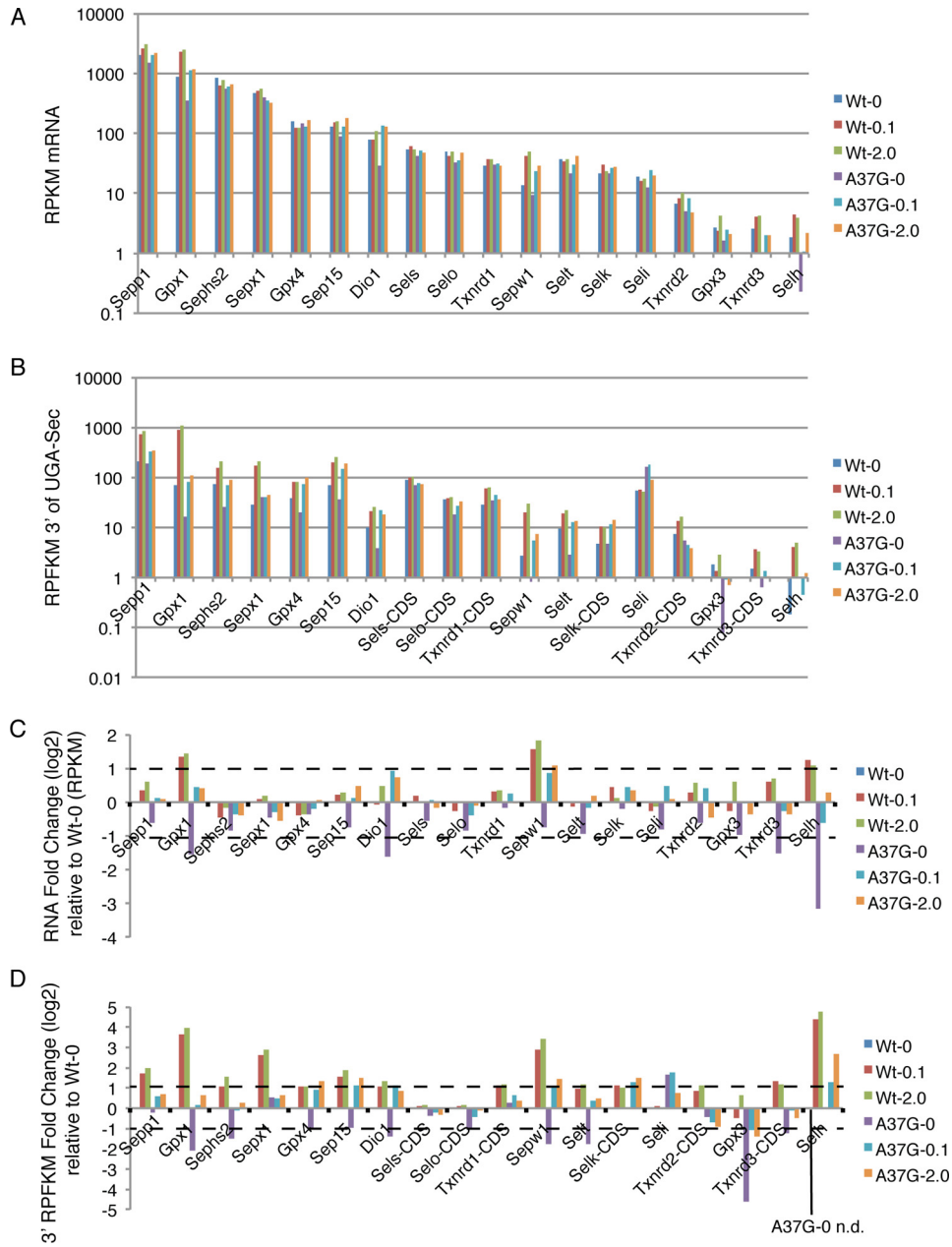

FIGURE 2. **Quantitative analysis of selenoprotein mRNA levels and ribosome footprints.** *A*, selenoprotein mRNA levels were determined by RNA abundance analysis (RPKM, RNA reads/kilobase/million mapped reads) of deep sequencing data for WT and *Trsp*^{A37G} mice (A37G) fed diets supplemented with 0, 0.1, or 2.0 ppm selenium. *B*, analysis was the same as *A* except for RPFKMs (ribosome footprint reads/kilobase/million mapped reads). RPFKMs were determined for all selenoproteins 3′ of the UGA-Sec codon with the exception of *Sels*, *Txnrd1*, *Selk*, *Selo*, *Txnrd2*, and *Txnrd3* that have UGA-Sec codons located near the C terminus. For these selenoproteins, CDS ribosome footprinting RPFKMs are reported (*Sels-CDS*, *Txnrd1-CDS*, *Selk-CDS*, *Selo-CDS*, *Txnrd2-CDS*, and *Txnrd3-CDS)*. *C*, analysis was the same as *A* and was expressed as the log2 changes in selenoprotein mRNA levels measured by RPKM relative to the corresponding values observed in WT selenium-deficient mice. *D*, analysis was the same as *B*, expressed as the log2 change in selenoprotein ribosome footprint RPFKM relative to the corresponding RPFKM values observed in selenium-deficient WT mice. *n.d.*, not determined.

gated region had RPKM or RPFKM values below a threshold value of 10 ("Experimental Procedures" and Ref. 26).

The selenoproteins revealed a range of 5′ TEs, with *Selt* and *Gpx4* having the highest TE across all dietary selenium levels in both WT and *Trsp*^{A37G} mice, whereas *Gpx1* and *Selk* are examples of selenoproteins with low 5′ TEs (Fig. 5*A*). The addition of 0.1 or 2.0 ppm selenium resulted in less than a 2-fold increase in 5′ TE relative to selenium-deficient WT mice with the exception of *Gpx1* in WT mice fed 2.0 ppm selenium diets, where the 5′ TE increased 2.6-fold, and for *Selk* in *Trsp*^{A37G} mice fed 0.1 and 2.0 ppm selenium diets, where the 5′ TE increased 2.3- and 2.4-fold, respectively (Fig. 5*C*). Furthermore, the 5′ TE of *Sepx1* in *Trsp*^{A37G} mice was reduced by 0.63-, 0.33-, and 0.37-fold compared with selenium-deficient WT mice, suggesting that the mcm5U isoform of Sec-tRNA$^{[Ser]Sec}$ may have an effect on either translation initiation or elongation rates upstream of the UGA-Sec codon of *Sepx1*.

In contrast to the relatively small changes in 5′ TE, a complex pattern of selenium-dependent changes in 3′ TE was observed reflecting changes in Sec incorporation efficiency depending on

both dietary selenium levels and Um34 methylation (Fig. 5, *B* and *D*). For all mRNAs examined with the exception of *Seli* in $Trsp^{A37G}$ mice, the 3′ TE was reduced compared with the 5′ TE, indicating that Sec incorporation is not 100% efficient (compare Fig. 5, *A* to *B*). In WT mice, the addition of selenium to the diet increased 3′ TEs for *Gpx1*, *Sepx1*, *Sepw1*, *Sepp1*, *Sephs2*, *Dio1* *Gpx4*, *Sep15*, and *Selt* from ~2-fold to nearly 8-fold (Fig. 5*D*). In contrast, we found the opposite effect for *Seli*, where the 3′ TE for *Seli* was slightly decreased in WT mice fed selenium-supplemented diets and increased under all selenium dietary levels in $Trsp^{A37G}$ mice (3.1-fold in diets with 0 ppm selenium, 2.4-fold with 0.1 ppm selenium, and 1.3-fold with 2.0 ppm selenium, compared with WT selenium-deficient mice). In the $Trsp^{A37G}$ mouse samples, three selenoprotein mRNAs, *Gpx4*, *Sep15*, and *Selt*, showed a selenium-dependent increase in 3′ TE to approximately the same levels as was observed in WT mice. In contrast, *Gpx1*, *Sepx1*, *Sepw1*, *Dio1*, *Sepp1*, and *Sephs2* showed a reduced response to dietary selenium supplementation in the $Trsp^{A37G}$ mouse samples, suggesting that translation of these four mRNAs requires Um34 methylation (to varying degrees) for efficient Sec incorporation and translational regulation by dietary selenium.

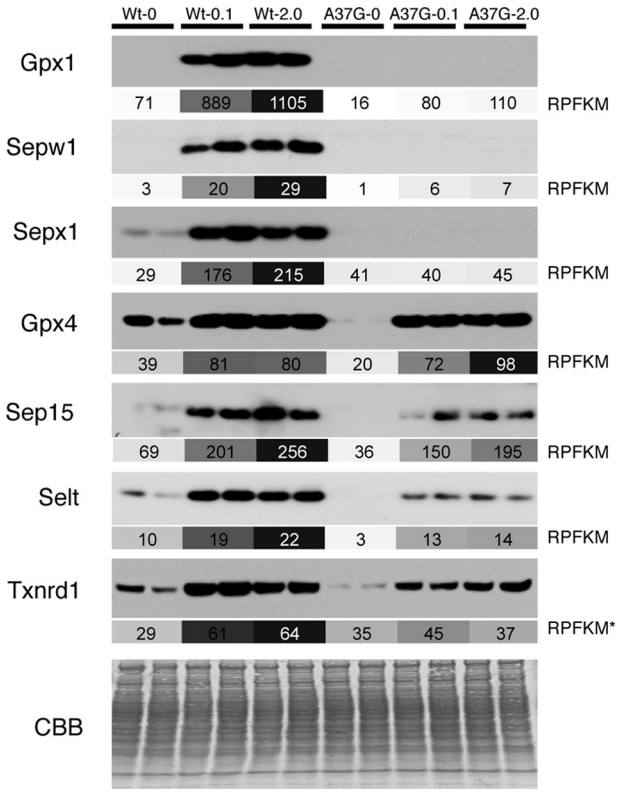

FIGURE 3. **Comparison of Western blots and ribosome profiling measurements of selenoprotein synthesis.** Western blots of Gpx1, Sepw1, Sepx1, Gpx4, Sep15, Selt, and Txnrd1 from two biological samples are shown *above the corresponding RPFKM* (ribosome footprint reads/kilobase/million mapped reads) values in *shaded boxes*. For each selenoprotein, RPFKM values are shaded according to a continuous scale from 0 RPFKM (*white*) to the highest RPFKM value for that gene (*dark gray*). RPFKM values are for the portion of the mRNA downstream of the UGA-Sec codon except for Txnrd1, where the RPFKM value is for the CDS (RPFKM*). *CBB*, Coomassie Blue staining.

Ribosome Density Near the UGA-Sec Codon and in the 5′-UTR—Slow decoding of UGA-Sec codons resulting in ribosome pausing has been postulated to be a kinetic feature of Sec incorporation (34, 39). Here we find little evidence of excess ribosome footprints near UGA-Sec codons with the notable exceptions of four selenoprotein mRNAs, *Gpx1*, *Sepx1*, *Sepw1*, and *Selh*, where the number of ribosome footprints either at the UGA codon or in the 5 preceding codons exceeded 20% of the total footprints mapping to the respective mRNA (Table 1). Fig. 6 shows the ribosome footprint coverage across the mRNA (Fig. 6, *A*, *C*, *E*, and *G*) and the A-site codon location (Fig. 6. *B*, *D*, *F*, and *H*) of ribosome footprints mapping near the UGA-Sec codon for these mRNAs. Only for *Sepx1* were there a large number of footprints with A-sites mapping to the UGA-Sec codon (Fig. 6*D*). The majority of footprints mapped to the −2 codon relative to the UGA-Sec codon for *Gpx1* (Fig. 6*B*) and to the −4 codon for *Sepw1* and *Selh* (Fig. 6, *F* and *H*).

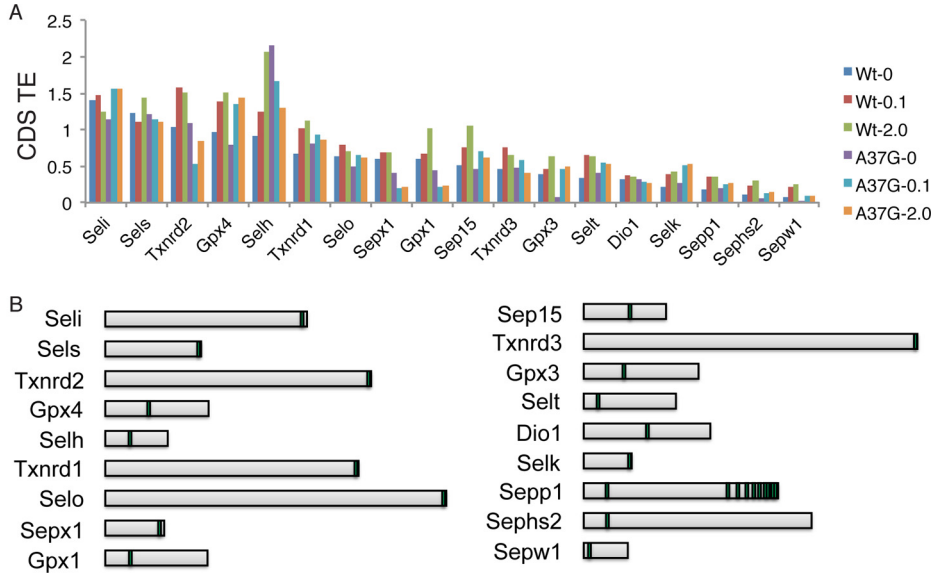

FIGURE 4. **Translational efficiency of selenoprotein coding sequences.** *A*, translational efficiency was calculated as the ribosome footprint RPFKMs/RNA RPKMs across each CDS for WT and $Trsp^{A37G}$ mice fed diets supplemented with 0, 0.1, or 2.0 ppm selenium diets. *B*, relative length and position of the UGA-Sec codon (*vertical bars*) are shown for each selenoprotein.

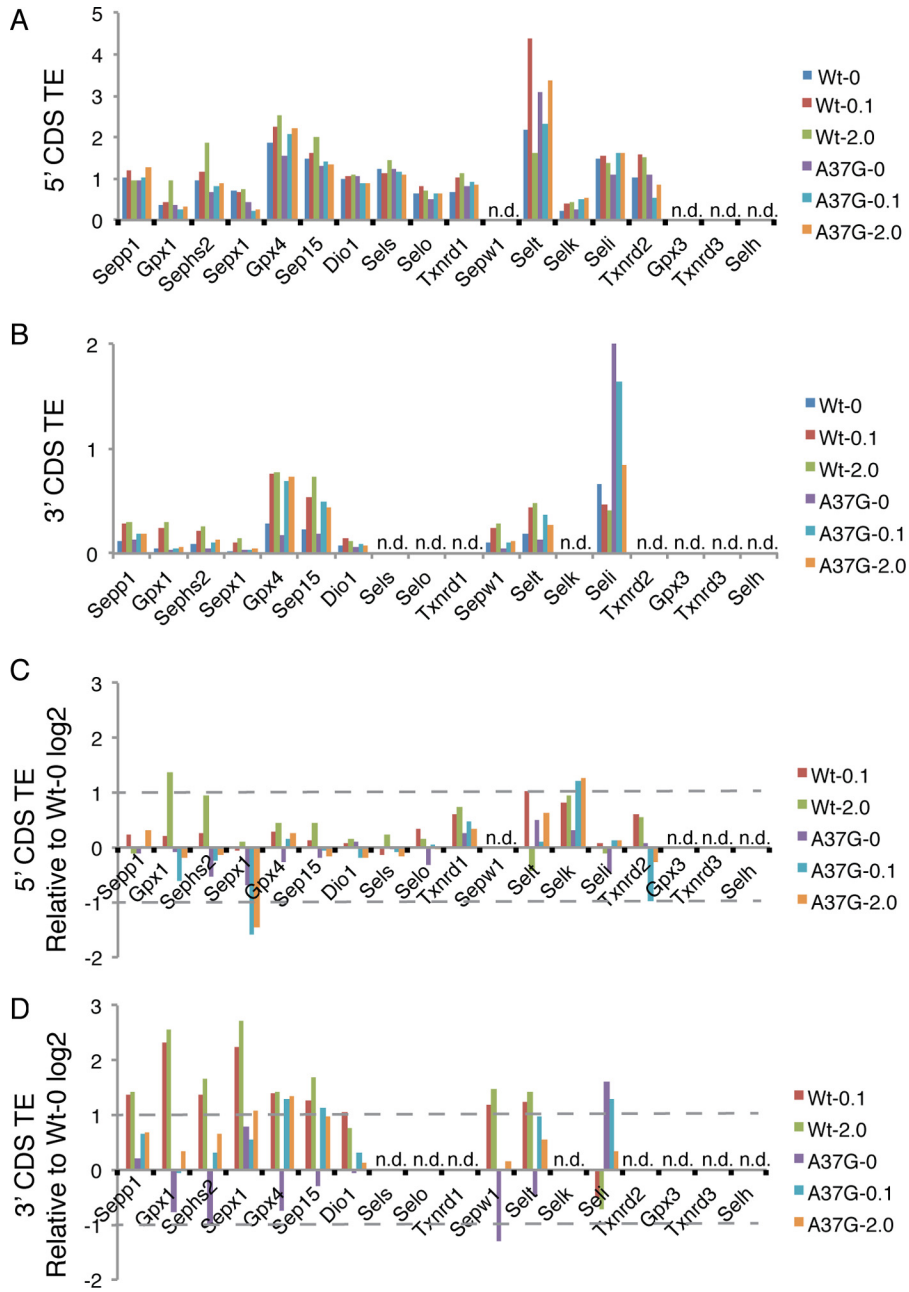

FIGURE 5. **Translational efficiency 5′ and 3′ of UGA-Sec codons.** Translational efficiency (RPFKM/RPKM) of selenoprotein-coding sequences located either 5′ (*A*) or 3′ (*B*) of UGA-Sec codon (5′ or 3′ of the first UGA-Sec codon for *Sepp1*) in samples from WT and $Trsp^{A37G}$ (A37G) mice fed diets supplemented with 0, 0.1, or 2.0 ppm selenium. *C*, same as *A*, expressed as the log 2 change in 5′ TE relative to the corresponding values measured in WT mice fed selenium-deficient diets. *D*, same as *B* expressed as the log 2 change in 3′ TE relative to the corresponding values measured in WT mice fed selenium-deficient diets. Selenoprotein mRNAs were excluded from this analysis (*n.d.*) if 5′ or 3′ RPFKM values were <10 in Wt-0.1 sample or if the UGA-Sec was located near the start (5′ TE) or stop codon (3′ TE).

To confirm accurate assignment of A-site codons, ribosome footprints were mapped to the *Xbp1* mRNA, which is known to have a translational pause site at Asn-256 (31, 40), and this site is found to be a predominant site of ribosome pausing in our experiment (supplemental Fig. S3). The A-site relative to AUG initiation codons and UGA termination codons of RefSeq mRNAs are also shown in supplemental Fig. S3. The A-site codons start abruptly at the +1 codon (the AUG is in the P-site during initiation) and stop at the codon immediately preceding UGA termination codons. Ribosome footprint size was also examined at UGA-Sec codons to determine if the size was altered in such a way that it might affect A-site assignment at UGA-Sec codons. The results show that altered footprint size was not skewed relative to the size of ribosome footprints at other CDS locations.

Finally, we observed elevated mRNA protection in the 5′-UTR of several selenoprotein mRNAs. The highest levels of 5′-UTR protection were observed for *Selh*, *Sephs2*, *Txnrd1*, and *Selt*, where the fraction approached or exceeded 10% that of the total ribosome-protected fragments mapping to each respective mRNA (Table 2). Ribosome footprint coverage of 5′-UTRs is shown for *Selh* (Fig. 6*G*) as well as *Sephs2* and *Selt* (Fig. 7).

TABLE 1

Fraction of ribosome footprints near UGA-Sec codons

The number of ribosome footprints with A-sites mapping near the UGA-Sec codon (−5 to +1 codons) is shown as a percentage of the total ribosome footprints mapping to each respective selenoprotein gene. Data are shown for WT or *Trsp*^{A37G} (A37G) mice fed diets supplemented with 0, 0.1, or 2.0 ppm selenium.

	Wt-0	Wt-0.1	Wt-2.0	A37G-0	A37G-0.1	A37G-2.0
Gpx1	80	64	68	86	71	64
Selh	38	36	49	50	54	58
Sepw1	34	26	27	35	23	36
Sepx1	31	42	32	37	30	29
Dio1	10	7	11	9	8	5
Gpx3	7	3	8	0	4	11
Selt	4	3	2	8	2	2
Sep15	3	3	4	7	4	2
Selk	3	2	1	6	4	4
Sepp1	2	1	2	3	2	1
Gpx4	2	2	2	1	2	3
Seli	2	2	1	3	1	2
Sephs2	1	1	2	2	1	1
Selo	1	1	1	1	1	1
Sels	1	2	2	1	1	2
Txnrd1	0	0	0	0	0	0
Txnrd2	0	0	0	0	0	0
Txnrd3	0	0	1	0	0	2

5′-UTR ribosome protection were also observed, albeit at low levels, for *Sepx1* (Fig. 6*C*), *Sep15*, *Selk*, and *Sepp1.*

DISCUSSION

Regulation of the selenoproteome by dietary selenium intake is a multifaceted process involving gene-specific changes in both mRNA abundance and ribosome activity (Fig. 1). We find that selenoprotein mRNA levels in WT mouse liver are relatively resistant to changing levels of dietary selenium with the notable exception of *Gpx1*, *Sepw1*, and *Selh* in both WT and *Trsp*^{A37G} mice as well as *Dio1* in selenium-deficient *Trsp*^{A37G} mice (Fig. 2 and supplemental Fig. S2). Although changes in transcriptional regulation by dietary selenium cannot be excluded as a contributing factor, we suggest that altered rates of mRNA turnover and, more specifically, susceptibility to NMD based on the efficiency of Sec insertion relative to translational termination at the UGA-Sec codon is the more likely explanation. In support of this notion are the observations that *Gpx1* is a known target of NMD (18, 41) with the degree of susceptibility to NMD depending upon selenium availability. Also, *Sepw1* mRNA abundance in rat L8 cells is affected by mRNA turnover, not transcription, when selenium levels are altered (42). *Dio1* may be an exceptional case, as a reduction in mRNA abundance was only observed in selenium-deficient *Trsp*^{A37G} mice. The three deiodinases in mammals (the other two deiodinases, *Dio2* and *Dio3*, were below detection limits in liver) are involved in the biosynthesis and interconversion of thyroid hormones between the inactive and active form, T4 and T3, respectively (43). As the *Dio1* gene contains thyroid hormone response promoter elements (44), it is a distinct possibility that altered levels of the active T3 hormone, due to changing deiodinase activity in liver or other tissues, may create a feedback loop affecting transcription of *Dio1* that may in part contribute to the large decrease in *Dio1* mRNA observed in selenium-deficient *Trsp*^{A37G} mice.

We find that the selenoprotein mRNAs in liver that reveal the largest changes in abundance due to altered dietary selenium levels (*Gpx1*, *Sepx1*, *Sepw1*, and *Selh*) are the same as those that reveal the greatest changes in active translation and Sec incorporation efficiency. The data presented in Fig. 5 further clarify the mechanism of translational control. Although selenium availability appears to have modest effects on translation initiation estimated by changing translational efficiency upstream of the UGA-Sec codon, we find dynamic selenium-dependent changes in ribosome density downstream of the UGA-Sec codon, supporting a model in which Sec incorporation is a limiting step during biosynthesis of selenoproteins and a primary target for selenium regulation of selenoprotein expression.

It has been previously reported that the selenium- induced methylation of Um34 is required for expression of a subset of stress-related selenoproteins (see Fig. 3 and Refs. 24 and 25). Here we extend these findings by showing that either selenium deficiency or expression of an A37G mutant of Sec-tRNA$^{[Ser]Sec}$ severely reduced ribosome density downstream of the UGA-Sec codon for *Gpx1*, *Sepx1*, *Sepw1*, and *Selh*, reflecting diminished Sec incorporation efficiency. In addition, under selenium-adequate conditions, Sec insertion efficiency remains relatively unaffected by expression of the A37G mutant Sec-tRNA$^{[Ser]Sec}$ for the housekeeping selenoprotein mRNAs, including *Gpx4* and *Sep15*, with many selenoproteins showing intermediate changes. *Seli* is notable among the selenoproteins in that selenium-adequate or -supplemented diets do not appear to increase Sec insertion efficiency in WT mice, whereas in *Trsp*^{A37G} mice Sec insertion efficiency is increased, suggesting the unexpected possibility that the unmethylated mcm5U Sec-tRNA$^{[Ser]Sec}$ isoform may be preferentially utilized for UGA-Sec decoding of *Seli*, thus increasing its expression under selenium- limiting conditions. It should be noted that the UGA-Sec codon is near the termination codon of *Seli*, and thus ribosome density 3′ of the UGA-Sec codon may also be influenced by the efficiency of termination. The Seli protein is a putative CDP-alcohol phosphatidyltransferase involved in the production of phospholipids (45), an activity that may be important for replacing damaged phospholipids due to oxidative stress induced by selenium deficiency.

Furthermore, we find evidence for a high level of ribosome protection immediately upstream of the UGA-Sec codons of *Gpx1*, *Sepx1*, *Sepw1*, and *Selh*, the same genes that are most affected by dietary selenium levels. Assignment of ribosome A-sites to the 3′ end of RefSeq mRNAs (supplemental Fig. S3) demonstrates a sharp drop-off at the codon preceding standard UGA termination codons. Consequently, the accumulation of ribosomes immediately upstream of UGA-Sec codons must be interpreted with caution. In one scenario, ribosomes may pause at the UGA-Sec codon due to slow decoding, resulting in tightly stacked ribosomes (34, 46) behind the UGA-Sec codon. If ribosomes decoding UGA-Sec codons are not effectively captured by cycloheximide treatment and are released during tissue processing, this could allow for limited movement of the preceding paused ribosomes to positions immediately upstream of the UGA-Sec codon. Alternatively, ribosome pausing may occur before the UGA-Sec codon enters the A-site of the ribosome. In this case, slow decoding of upstream codons could allow time for assembly of the Sec incorporation machinery and reprogramming of ribosomes before decoding of the UGA-Sec codon, thus minimizing competition with termination. Several

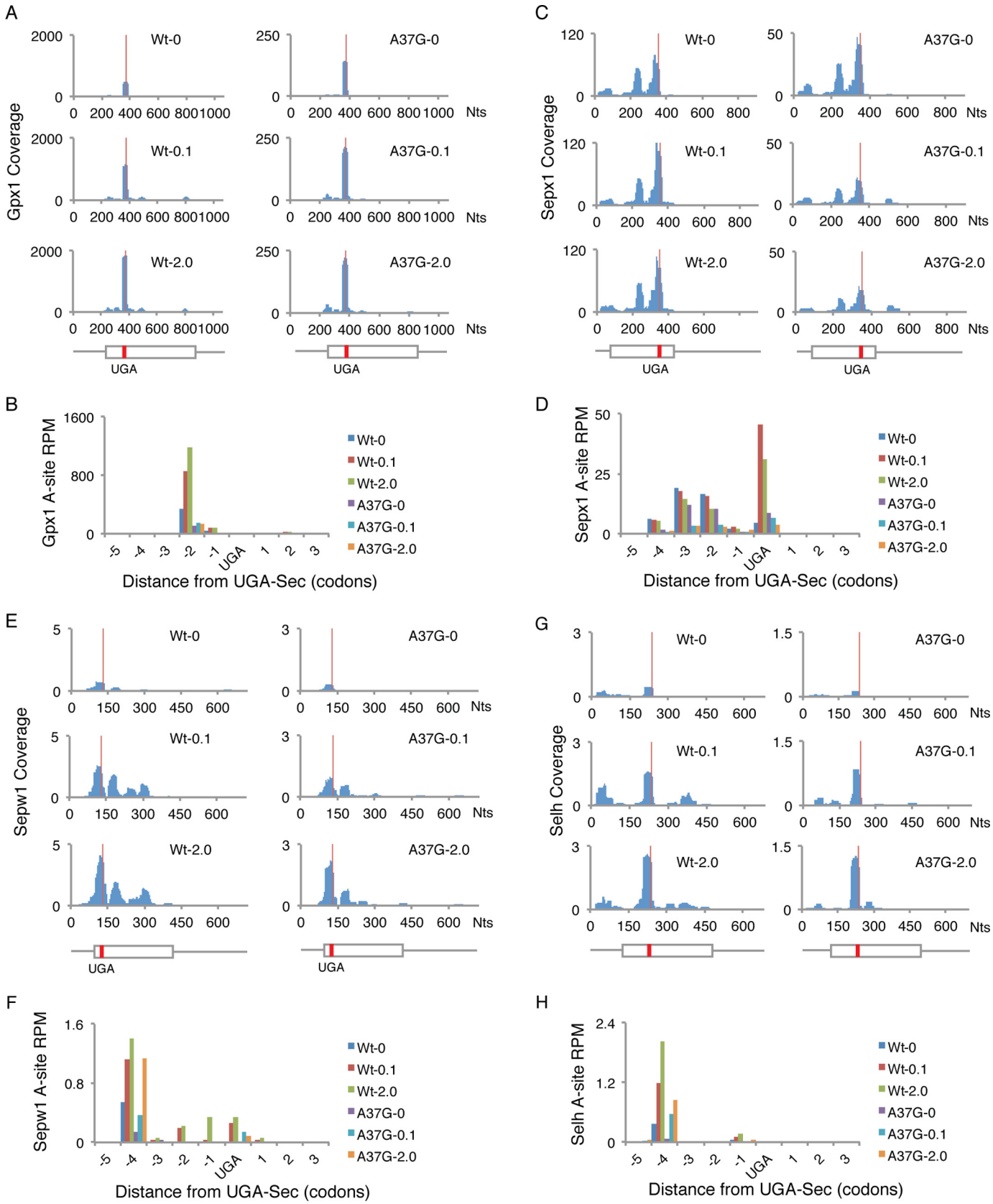

FIGURE 6. **Ribosome footprints near UGA-Sec codons.** The number of ribosome footprints mapping to each nucleotide across the mRNAs of *Gpx1* (*A*), *Sepx1* (*C*), *Sepw1* (*E*), and *Selh* (*G*) normalized to total mapped reads (*Coverage*) is shown for each mRNA in livers of WT or $Trsp^{A37G}$ (*A37G*) mice fed diets supplemented with 0, 0.1, or 2.0 ppm selenium. *Below the histograms in A*, *C*, *E*, and *G* is a schematic of each mRNA. *Thin lines* represent UTRs, *boxes* represent open reading frames, and *red lines* indicate the position of the UGA-Sec codons. The number of ribosome footprints with A-site codons assigned to the −5 to +3 codons relative to UGA-Sec, normalize to total mapped reads (reads per million mapped reads, rpm, is shown for *Gpx1* (*B*), *Sepx1* (*D*), *Sepw1* (*F*), and *Selh* (*H*).

previous studies have demonstrated that secondary structures downstream of UGA-Sec codons, which may slow local ribosome elongation rates, enhance Sec incorporation efficiency (47, 48). In addition, nascent peptides in the exit channel of the ribosome may provide an alternative mechanism to slow translation in the region preceding the UGA-Sec codon. Furthermore, additional caution is warranted due to library construction biases that may influence quantification of ribosome-protected fragments at any given position. Nevertheless, experimental analysis of the UGA-Sec sequence context of these mRNAs is warranted to illuminate the mechanisms contributing to increased ribosome protection and its contribution to selenium-dependent regulation of Sec incorporation during synthesis of these selenoproteins.

TABLE 2

Fraction of ribosome footprints in 5′-UTRs

The number of ribosome footprints with A-sites mapping within the 5′-UTR (excluding the two codons preceding the AUG codon) are shown as a percentage of the total ribosome footprints mapping to each respective selenoprotein gene. Data are shown for WT or *Trsp*^{A37G} (A37G) mice fed diets supplemented with 0, 0.1, or 2.0 ppm selenium.

	Wt-0	Wt-0.1	Wt-2.0	A37G-0	A37G-0.1	A37G-2.0
Gpx1	0	0	0	0	0	0
Selh	42	33	17	38	16	11
Sepw1	13	2	4	0	6	5
Sepx1	5	4	5	4	4	5
Dio1	0	0	0	0	0	0
Gpx3	0	0	0	0	0	0
Selt	9	8	13	8	8	10
Sep15	4	2	1	4	2	1
Selk	6	8	7	1	8	7
Sepp1	7	4	5	5	4	4
Gpx4	0	0	0	0	0	0
Seli	1	1	2	1	1	1
Sephs2	33	19	18	31	25	23
Selo	0	0	0	0	0	0
Sels	0	0	0	0	0	0
Txnrd1	10	10	14	3	6	10
Txnrd2	0	0	0	0	0	0
Txnrd3	3	0	0	0	0	0

Increased ribosome protection was observed in the 5′-UTRs of several selenoproteins. For *Selh*, *Sephs2*, and *Selt*, a contiguous open reading frame exists between the 5′-UTR footprints and the annotated AUG codons, suggesting the possibility of N-terminal extensions to the selenoprotein or, alternatively, translation of peptides derived from small out-of-frame upstream upstream open reading frames. Extensive genome-wide translation of upstream open reading frames, initiated by both AUG and non-AUG codons, has recently been described in studies utilizing ribosome profiling in mammalian cells and in yeast (29–31). Although the fraction of total ribosome-protected fragments mapping to the 5′-UTR did have an inverse correlation with dietary selenium levels for *Selh* and *Sephs2* in our experiments (Table 2), the relationship between 5′-UTR translation and selenium-dependent regulation of these selenoproteins remains unclear, and the effect is likely to be small based on our observation that 5′ TE, which should in part reflect initiation efficiency, is relatively unaffected by increasing selenium availability. Given the complex relationship between 5′-UTR translation and gene translation, it is possible that 5′-UTR translation is not related to dietary selenium levels but is utilized under other circumstances to regulate selenoprotein translation or to produce selenoproteins with N-terminal extensions.

The data presented here demonstrate that dietary selenium levels can alter the efficiency by which the standard rules of genetic decoding are redefined to allow UGA codons to encode Sec. Importantly, we show that UGA-Sec redefinition is inefficient and a primary determinant of selenoprotein synthesis rates *in vivo*. Our study provides direct support for a model in which the mcm^{5}U and mcm^{5}Um isoforms of Sec-tRNA$^{[Ser]Sec}$ are differentially utilized to determine Sec incorporation efficiencies in a manner that depends upon the selenoprotein mRNA. Likely candidates for factors involved in discrimination between the two Sec-tRNA$^{[Ser]Sec}$ isoforms include differences

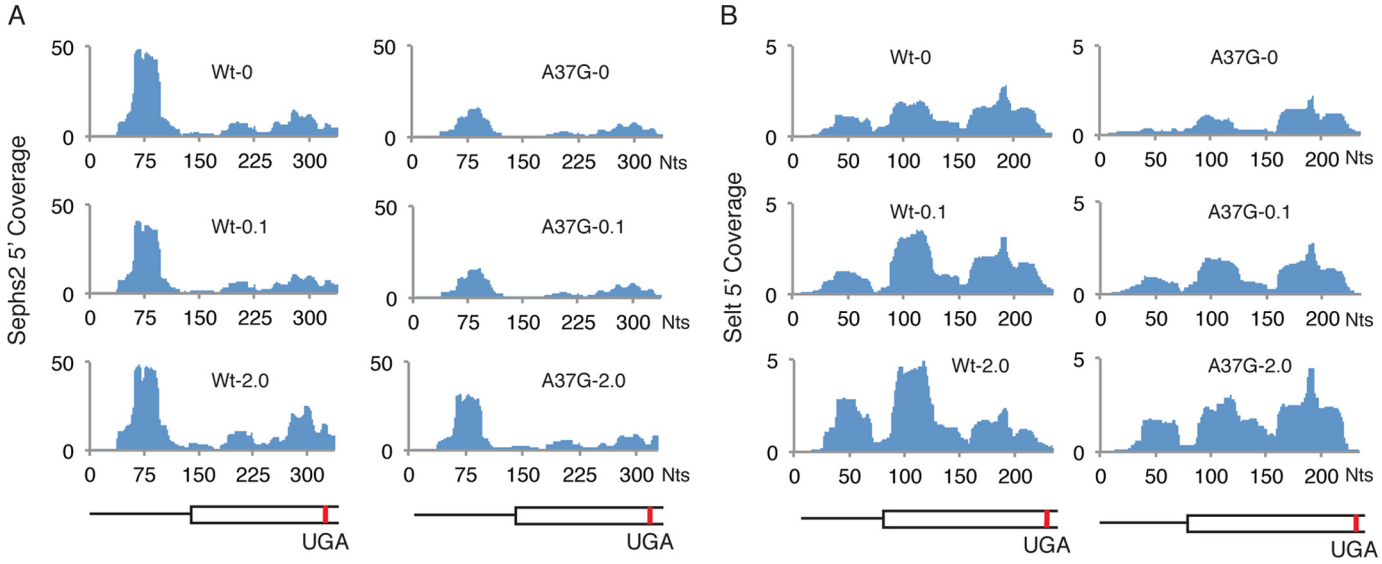

FIGURE 7. **Ribosome protection in the 5′-UTR.** The number of ribosome footprints mapping to each nucleotide across the 5′-UTR and coding sequence extending 10 nt beyond the UGA-Sec codon of *Sephs2* (*A*) and *Selt* (*B*), normalized to total mapped reads (*Coverage*) is shown for each mRNA in livers of WT or *Trsp*^{A37G} (*A37G*) mice fed diets supplemented with 0, 0.1, or 2.0 ppm selenium. *Below the histograms in A* and *B* is a schematic of each mRNA. *Thin lines* represent the 5′-UTR, and *boxed regions* are the open reading frame up to, and extending 10 nt beyond the UGA-Sec codon. *Red lines* indicate the position of the UGA-Sec codon.

between SECIS elements, the local sequence context of the UGA-Sec codon, and their influence on either recruitment of Sec-tRNA$^{[Ser]Sec}$ isoform-specific eEFSec ternary complexes or isoform-specific recognition of the UGA-Sec codon. The efficiency of Sec insertion relative to termination for each selenoprotein mRNA further impacts mRNA turnover rate and abundance. As dietary selenium levels determine the ratio of mcm^{5}U and mcm^{5}Um Sec-tRNA$^{[Ser]Sec}$ isoforms (23), the preferential utilization of one isoform over the other and the resulting effect of altered Sec insertion efficiency on mRNA abundance provides a unifying mechanism to explain how dietary selenium regulates the readout of the genetic code and gene-specific selenoprotein expression.

Acknowledgments—We thank Drs. Ray Gesteland and John Atkins (University of Utah) for helpful discussions and Dr. Brian Dalley (University of Utah) for assistance with library construction and deep sequence.

REFERENCES

1. Keshan, Disease Research Group (1979) Epidemiologic studies on the etiologic relationship of selenium and Keshan disease. *Chin. Med. J.* **92,** 477–482
2. Yang, G. Q., Wang, S. Z., Zhou, R. H., and Sun, S. Z. (1983) Endemic selenium intoxication of humans in China. *Am. J. Clin. Nutr.* **37,** 872–881
3. Nuttall, K. L. (2006) Evaluating selenium poisoning. *Ann. Clin. Lab. Sci.* **36,** 409–420
4. Hatfield, D., Berry, MJ, Gladyshev, VN (ed) (2012) *Selenium*: *Its Molecular Biology and Role in Human Health*, Springer-Verlag New York Inc., New York
5. Kryukov, G. V., Castellano, S., Novoselov, S. V., Lobanov, A. V., Zehtab, O., Guigó, R., and Gladyshev, V. N. (2003) Characterization of mammalian selenoproteomes. *Science* **300,** 1439–1443
6. Mariotti, M., Ridge, P. G., Zhang, Y., Lobanov, A. V., Pringle, T. H., Guigo, R., Hatfield, D. L., and Gladyshev, V. N. (2012) Composition and evolution of the vertebrate and mammalian selenoproteomes. *PLoS ONE* **7,** e33066
7. Berry, M. J., Banu, L., Chen, Y. Y., Mandel, S. J., Kieffer, J. D., Harney, J. W., and Larsen, P. R. (1991) Recognition of UGA as a selenocysteine codon in type I deiodinase requires sequences in the 3′ untranslated region. *Nature* **353,** 273–276
8. Berry, M. J., Banu, L., Harney, J. W., and Larsen, P. R. (1993) Functional characterization of the eukaryotic SECIS elements which direct selenocysteine insertion at UGA codons. *EMBO J.* **12,** 3315–3322
9. Hill, K. E., Lloyd, R. S., and Burk, R. F. (1993) Conserved nucleotide sequences in the open reading frame and 3′ untranslated region of selenoprotein P mRNA. *Proc. Natl. Acad. Sci. U.S.A.* **90,** 537–541
10. Shen, Q., Chu, F. F., and Newburger, P. E. (1993) Sequences in the 3′-untranslated region of the human cellular glutathione peroxidase gene are necessary and sufficient for selenocysteine incorporation at the UGA codon. *J. Biol. Chem.* **268,** 11463–11469
11. Copeland, P. R., and Driscoll, D. M. (1999) Purification, redox sensitivity, and RNA binding properties of SECIS-binding protein 2, a protein involved in selenoprotein biosynthesis. *J. Biol. Chem.* **274,** 25447–25454
12. Berry, M. J., Tujebajeva, R. M., Copeland, P. R., Xu, X. M., Carlson, B. A., Martin, G. W., 3rd, Low, S. C., Mansell, J. B., Grundner-Culemann, E., Harney, J. W., Driscoll, D. M., and Hatfield, D. L. (2001) Selenocysteine incorporation directed from the 3′UTR. Characterization of eukaryotic EFsec and mechanistic implications. *Biofactors* **14,** 17–24
13. Fagegaltier, D., Hubert, N., Yamada, K., Mizutani, T., Carbon, P., and Krol, A. (2000) Characterization of mSelB, a novel mammalian elongation factor for selenoprotein translation. *EMBO J.* **19,** 4796–4805
14. Hadley, K. B., and Sunde, R. A. (2001) Selenium regulation of thioredoxin reductase activity and mRNA levels in rat liver. *J. Nutr. Biochem.* **12,** 693–702
15. Hill, K. E., Lyons, P. R., and Burk, R. F. (1992) Differential regulation of rat liver selenoprotein mRNAs in selenium deficiency. *Biochem. Biophys. Res. Commun.* **185,** 260–263
16. Lei, X. G., Evenson, J. K., Thompson, K. M., and Sunde, R. A. (1995) Glutathione peroxidase and phospholipid hydroperoxide glutathione peroxidase are differentially regulated in rats by dietary selenium. *J. Nutr.* **125,** 1438–1446
17. Christensen, M. J., and Burgener, K. W. (1992) Dietary selenium stabilizes glutathione peroxidase mRNA in rat liver. *J. Nutr.* **122,** 1620–1626
18. Moriarty, P. M., Reddy, C. C., and Maquat, L. E. (1998) Selenium deficiency reduces the abundance of mRNA for selenium-dependent glutathione peroxidase 1 by a UGA-dependent mechanism likely to be nonsense codon-mediated decay of cytoplasmic mRNA. *Mol. Cell. Biol.* **18,** 2932–2939
19. Weiss, S. L., and Sunde, R. A. (1998) Cis-acting elements are required for selenium regulation of glutathione peroxidase-1 mRNA levels. *RNA* **4,** 816–827
20. Budiman, M. E., Bubenik, J. L., Miniard, A. C., Middleton, L. M., Gerber, C. A., Cash, A., and Driscoll, D. M. (2009) Eukaryotic initiation factor 4a3 is a selenium-regulated RNA-binding protein that selectively inhibits selenocysteine incorporation. *Mol. Cell* **35,** 479–489
21. Low, S. C., Grundner-Culemann, E., Harney, J. W., and Berry, M. J. (2000) SECIS-SBP2 interactions dictate selenocysteine incorporation efficiency and selenoprotein hierarchy. *EMBO J.* **19,** 6882–6890
22. Squires, J. E., Stoytchev, I., Forry, E. P., and Berry, M. J. (2007) SBP2 binding affinity is a major determinant in differential selenoprotein mRNA translation and sensitivity to nonsense-mediated decay. *Mol. Cell. Biol.* **27,** 7848–7855
23. Diamond, A. M., Choi, I. S., Crain, P. F., Hashizume, T., Pomerantz, S. C., Cruz, R., Steer, C. J., Hill, K. E., Burk, R. F., and McCloskey, J. A. (1993) Dietary selenium affects methylation of the wobble nucleoside in the anticodon of selenocysteine tRNA$^{[Ser]Sec}$. *J. Biol. Chem.* **268,** 14215–14223
24. Moustafa, M. E., Carlson, B. A., El-Saadani, M. A., Kryukov, G. V., Sun, Q. A., Harney, J. W., Hill, K. E., Combs, G. F., Feigenbaum, L., Mansur, D. B., Burk, R. F., Berry, M. J., Diamond, A. M., Lee, B. J., Gladyshev, V. N., and Hatfield, D. L. (2001) Selective inhibition of selenocysteine tRNA maturation and selenoprotein synthesis in transgenic mice expressing isopentenyladenosine-deficient selenocysteine tRNA. *Mol. Cell. Biol.* **21,** 3840–3852
25. Carlson, B. A., Xu, X. M., Gladyshev, V. N., and Hatfield, D. L. (2005) Selective rescue of selenoprotein expression in mice lacking a highly specialized methyl group in selenocysteine tRNA. *J. Biol. Chem.* **280,** 5542–5548
26. Carlson, B. A., Moustafa, M. E., Sengupta, A., Schweizer, U., Shrimali, R., Rao, M., Zhong, N., Wang, S., Feigenbaum, L., Lee, B. J., Gladyshev, V. N., and Hatfield, D. L. (2007) Selective restoration of the selenoprotein population in a mouse hepatocyte selenoproteinless background with different mutant selenocysteine tRNAs lacking Um34. *J. Biol. Chem.* **282,** 32591–32602
27. Langmead, B., Trapnell, C., Pop, M., and Salzberg, S. L. (2009) Ultrafast and memory-efficient alignment of short DNA sequences to the human genome. *Genome Biol* **10,** R25
28. Shrimali, R. K., Irons, R. D., Carlson, B. A., Sano, Y., Gladyshev, V. N., Park, J. M., and Hatfield, D. L. (2008) Selenoproteins mediate T cell immunity through an antioxidant mechanism. *J. Biol. Chem.* **283,** 20181–20185
29. Gerashchenko, M. V., Lobanov, A. V., and Gladyshev, V. N. (2012) Genome-wide ribosome profiling reveals complex translational regulation in response to oxidative stress. *Proc. Natl. Acad. Sci. U.S.A.* **109,** 17394–17399
30. Ingolia, N. T., Ghaemmaghami, S., Newman, J. R., and Weissman, J. S. (2009) Genome-wide analysis *in vivo* of translation with nucleotide resolution using ribosome profiling. *Science* **324,** 218–223
31. Ingolia, N. T., Lareau, L. F., and Weissman, J. S. (2011) Ribosome profiling of mouse embryonic stem cells reveals the complexity and dynamics of mammalian proteomes. *Cell* **147,** 789–802
32. Arava, Y., Boas, F. E., Brown, P. O., and Herschlag, D. (2005) Dissecting eukaryotic translation and its control by ribosome density mapping. *Nucleic Acids Res.* **33,** 2421–2432

33. Hendrickson, D. G., Hogan, D. J., McCullough, H. L., Myers, J. W., Herschlag, D., Ferrell, J. E., and Brown, P. O. (2009) Concordant regulation of translation and mRNA abundance for hundreds of targets of a human microRNA. *PLoS Biol.* **7,** e1000238
34. Fletcher, J. E., Copeland, P. R., and Driscoll, D. M. (2000) Polysome distribution of phospholipid hydroperoxide glutathione peroxidase mRNA. Evidence for a block in elongation at the UGA/selenocysteine codon. *RNA* **6,** 1573–1584
35. Nasim, M. T., Jaenecke, S., Belduz, A., Kollmus, H., Flohé, L., and McCarthy, J. E. (2000) Eukaryotic selenocysteine incorporation follows a nonprocessive mechanism that competes with translational termination. *J. Biol. Chem.* **275,** 14846–14852
36. Kim, L. K., Matsufuji, T., Matsufuji, S., Carlson, B. A., Kim, S. S., Hatfield, D. L., and Lee, B. J. (2000) Methylation of the ribosyl moiety at position 34 of selenocysteine tRNA$^{[Ser]Sec}$ is governed by both primary and tertiary structure. *Rna* **6,** 1306–1315
37. Kim, J. Y., Carlson, B. A., Xu, X. M., Zeng, Y., Chen, S., Gladyshev, V. N., Lee, B. J., and Hatfield, D. L. (2011) Inhibition of selenocysteine tRNA$^{[Ser]Sec}$ aminoacylation provides evidence that aminoacylation is required for regulatory methylation of this tRNA. *Biochem. Biophys. Res. Commun.* **409,** 814–819
38. Mortazavi, A., Williams, B. A., McCue, K., Schaeffer, L., and Wold, B. (2008) Mapping and quantifying mammalian transcriptomes by RNA-Seq. *Nat Methods* **5,** 621–628
39. Stoytcheva, Z., Tujebajeva, R. M., Harney, J. W., and Berry, M. J. (2006) Efficient incorporation of multiple selenocysteines involves an inefficient decoding step serving as a potential translational checkpoint and ribosome bottleneck. *Mol. Cell. Biol.* **26,** 9177–9184
40. Yanagitani, K., Imagawa, Y., Iwawaki, T., Hosoda, A., Saito, M., Kimata, Y., and Kohno, K. (2009) Cotranslational targeting of XBP1 protein to the membrane promotes cytoplasmic splicing of its own mRNA. *Mol. Cell* **34,** 191–200
41. Sunde, R. A., and Raines, A. M. (2011) Selenium regulation of the selenoprotein and nonselenoprotein transcriptomes in rodents. *Adv. Nutr.* **2,** 138–150
42. Gu, Q. P., Ream, W., and Whanger, P. D. (2002) Selenoprotein W gene regulation by selenium in L8 cells. *Biometals* **15,** 411–420
43. Bianco, A. C., Salvatore, D., Gereben, B., Berry, M. J., and Larsen, P. R. (2002) Biochemistry, cellular, and molecular biology, and physiological roles of the iodothyronine selenodeiodinases. *Endocr. Rev.* **23,** 38–89
44. Toyoda, N., Zavacki, A. M., Maia, A. L., Harney, J. W., and Larsen, P. R. (1995) A novel retinoid X receptor-independent thyroid hormone response element is present in the human type 1 deiodinase gene. *Mol. Cell. Biol.* **15,** 5100–5112
45. Horibata, Y., and Hirabayashi, Y. (2007) Identification and characterization of human ethanolaminephosphotransferase1. *J. Lipid Res.* **48,** 503–508
46. Wolin, S. L., and Walter, P. (1988) Ribosome pausing and stacking during translation of a eukaryotic mRNA. *EMBO J.* **7,** 3559–3569
47. Howard, M. T., Aggarwal, G., Anderson, C. B., Khatri, S., Flanigan, K. M., and Atkins, J. F. (2005) Recoding elements located adjacent to a subset of eukaryal selenocysteine-specifying UGA codons. *EMBO J.* **24,** 1596–1607
48. Howard, M. T., Moyle, M. W., Aggarwal, G., Carlson, B. A., and Anderson, C. B. (2007) A recoding element that stimulates decoding of UGA codons by Sec tRNA$^{[Ser]Sec}$. *RNA* **13,** 912–920